

# Synthesis and optical properties of ZnS nanoparticles decorated on SiO<sub>2</sub> nanospheres

Bui Hong Van\*, Nguyen Thi Bao Yen, Doan Thi Kim Dung, Hoang Chi Hieu



Use your smartphone to scan this QR code and download this article

## ABSTRACT

**Introduction:** In this study, ZnS nanoparticles were decorated on SiO<sub>2</sub> nanospheres via coprecipitation and the Stöber method. **Methods:** The materials were studied by X-ray diffraction (XRD), nano scanning electron microscopy (SEM), and photoluminescence spectra (PL). **Results:** ZnS nanoparticles exhibit a sphalerite structure with an average particle size of 2.8 nm and SiO<sub>2</sub> in the form of 115 nm nanospheres. The absorption spectrum of these nanoparticles displays a prominent band peaking at 320 nm. Additionally, at 300 K, the PL spectrum of ZnS reveals a broad band, comprising two component bands with peaks at 470 nm and 491 nm, attributed to lattice defects such as zinc and sulfur vacancies, interstitials, and surface states. Upon decorating ZnS nanoparticles on the surface of SiO<sub>2</sub> nanospheres, the UV-Vis absorption and PL spectra of ZnS shift toward longer wavelengths. The maximum peak of the UV-vis spectrum shifted from 322 to 328 nm, and two bands in the PL spectrum slightly changed to 472 and 494 nm. **Conclusion:** The shifts in the UV-vis and PL spectra are due to alterations in the surface states of the ZnS nanoparticles induced by the presence of SiO<sub>2</sub>. From the dependence of the PL spectra of ZnS nanoparticles and SiO<sub>2</sub>-decorated ZnS on the measured temperature from 10 to 300 K, the activation energies of ZnS and SiO<sub>2</sub>-decorated SiO<sub>2</sub> were estimated to be 38 and 40 meV, respectively.

**Key words:** ZnS, nanoparticle, ZnS-SiO<sub>2</sub>, absorption, photoluminescence

## 1 INTRODUCTION

Semiconductor nanomaterials have garnered extensive attention due to their vast potential applications, including catalysis, photonics, nonlinear optical devices, light-emitting diodes, flat displays, and infrared windows<sup>1-6</sup>. Nanostructured materials exhibit novel optical properties owing to the quantum size effect, making the precise control of their size a significant challenge in research and manufacturing. ZnS is one of the most critical and representative semiconductors, prompting various efforts to manipulate its optical properties. Techniques such as doping with elements such as Mn and Cu, employing polymer capping, and fabricating core/shell structures with materials such as ZnO and SiO<sub>2</sub> have been explored<sup>7-13</sup>. Silicon dioxide (SiO<sub>2</sub>)-based core shell particles have been widely studied because of their chemical inertness, ability to act as stabilizers, and ability to prevent particle coalescence. Their nanostructures can be homogeneously prepared and uniformly dispersed in different solutions. Due to its high biocompatibility and functionalized surface, SiO<sub>2</sub> readily binds to pigments, metal ions, and biomolecules<sup>14</sup>. Combining ZnS with SiO<sub>2</sub> holds tremendous potential for applications in photocatalysis, environmental treatment, and enhancing PL<sup>15</sup>.

SiO<sub>2</sub>@ZnS core-shell nanoparticles have been synthesized by various reported methods. For example, SiO<sub>2</sub>@ZnS core-shell nanoparticles were synthesized by a thermal decomposition approach by Jatin Mahajan et al.<sup>15</sup>. Ethiraj et al. synthesized SiO<sub>2</sub>@ZnS with thioglycerol molecules attached to functionalised silica particles<sup>16</sup>. Dhas et al. synthesized SiO<sub>2</sub>@ZnS core-shell nanoparticles using ultrasonic irradiation<sup>17</sup>, and Velikov et al. synthesized fluorescein isothiocyanate-incorporated SiO<sub>2</sub>@ZnS core-shell nanoparticles by combining homogeneous precipitation and thermal decomposition methods<sup>18</sup>. These reports analyzed the microstructure, morphology and UV-Vis absorption spectra of SiO<sub>2</sub>@ZnS core-shell nanoparticles, but studies on the luminescence spectra have not been discussed in detail. With the process of ZnS decoration on SiO<sub>2</sub>, defects and surface states in ZnS will be generated; therefore, the crystal structure and optical properties of ZnS will be affected. In this paper, we present the facile synthesis of ZnS nanoparticles decorated on SiO<sub>2</sub> nanospheres and demonstrate the influence of SiO<sub>2</sub> on the crystal structure, UV-Vis spectrum and PL spectra of ZnS nanoparticles from 10 to 300 K.

Faculty of Physics, VNU University of Science, Vietnam National University - Hanoi

## Correspondence

Bui Hong Van, Faculty of Physics, VNU University of Science, Vietnam National University - Hanoi

Email: buihongvan2011@gmail.com

## History

- Received:
- Accepted:
- Published Online:

## DOI :



Check for updates

## Copyright

© VNUHCM Press. This is an open-access article distributed under the terms of the Creative Commons Attribution 4.0 International license.



Cite this article : Van B H, Yen N T B, Dung D T K, Hieu H C. Synthesis and optical properties of ZnS nanoparticles decorated on SiO<sub>2</sub> nanospheres. *Sci. Tech. Dev. J.* 2024; (1):1-6.

## MATERIALS AND METHODS

Tetraethoxysilane (TEOS), Si(OC<sub>2</sub>H<sub>5</sub>)<sub>4</sub> (99,98%), (3-aminopropyl) trimethoxysilane (APTMS) (99,00%), zinc acetate Zn(CH<sub>3</sub>COO)<sub>2</sub>·2 H<sub>2</sub>O (99,99%), thioacetamide (TAA), CH<sub>3</sub>CSNH<sub>2</sub> (99%), ammonium NH<sub>3</sub> (25%), and absolute ethanol were purchased from Sigma Aldrich, China. All chemicals used were of analytical grade. Deionized (DI) water was used in all experiments.

ZnS nanoparticles were synthesized by a coprecipitation method from solutions of 0.01 M TAA and 0.01 M zinc acetate according to the following process: 30 ml of 0.01 M TAA solution was slowly added to 30 ml of 0.01 M zinc acetate solution, and the mixture was stirred for 2 hours to obtain a white precipitate. The white precipitate was centrifuged and filtered 3 times and then dried at 80°C for 15 hours to obtain ZnS powder. SiO<sub>2</sub> nanospheres were synthesized by the Stöber method from TEOS, NH<sub>3</sub> and absolute ethanol. ZnS (0.02 g), SiO<sub>2</sub> (0.1 g), APTMS (0.2 ml), DI water (40 ml) and absolute ethanol (10 ml) were mixed with magnetic stirring for 5 hours. The mixture was centrifuged and dried at 80°C for 15 hours to obtain ZnS nanoparticles decorated on SiO<sub>2</sub> nanospheres (denoted as SiO<sub>2</sub>@ZnS).

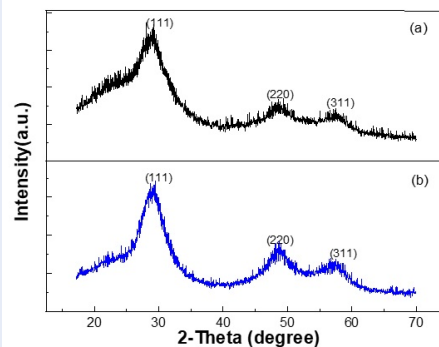
The microstructure and morphology of ZnS and SiO<sub>2</sub>@ZnS were investigated by a PANalytical Empyrean X-ray diffractometer using CuK $\alpha$  radiation ( $\lambda = 1.54056 \text{ \AA}$ ,  $2\theta = 10\text{--}70^\circ$ ) and a scanning electron microscope (FEI NOVA NANOSEM 450). UV-vis absorption spectra were recorded on a UV-2450 spectrometer (Shimadzu). The PL spectra were excited by 325 nm radiation from the He-Cd laser and recorded on a Spectra Pro2500 spectrometer (Priceton Instruments). The sample was cooled by an HC-4A air-cooled helium compressor (Sumitomo Heavy Industries).

## RESULTS AND DISCUSSION

### Structure and morphology of ZnS nanoparticles and SiO<sub>2</sub>@ZnS

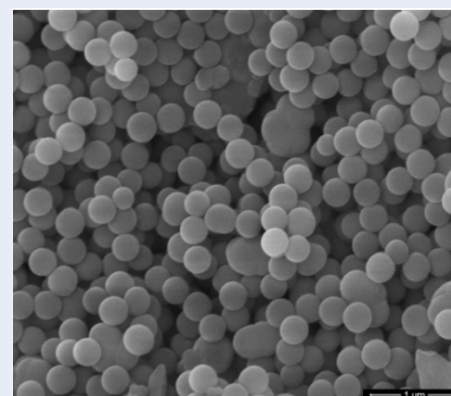
Figure 1a shows the XRD pattern of the ZnS nanoparticles (NPs). The diffraction peaks at  $23.91^\circ$ ,  $48.11^\circ$ , and  $57.11^\circ$  are attributed to the (111), (220), and (311) atomic planes of ZnS, respectively (according to PDF No. 96-500-0089). The existence of these peaks indicates that as-ZnS is a single-phase, cubic structure belonging to the symmetry group. The XRD pattern of SiO<sub>2</sub>@ZnS also shows peaks at  $23.91^\circ$ ,  $48.11^\circ$ , and  $57.11^\circ$ , similar to the XRD pattern of ZnS nanoparticles (Figure 1b). This indicates that as-SiO<sub>2</sub> does not affect the structure of ZnS when ZnS is decorated

on SiO<sub>2</sub>. From the XRD patterns and the Debye-Scherrer formula,  $D = \frac{0.9\lambda}{\beta \cos \theta}$  where D is the crystalline size,  $\lambda$  is the wavelength of CuK $\alpha$  radiation ( $1.54056 \text{ \AA}$ ),  $\beta$  is the full width at half maximum and  $\theta$  is the Bragg diffraction angle, the crystalline size of ZnS was calculated to be approximately 2.8 nm using a highly intense Bragg peak at  $23.91^\circ$ .



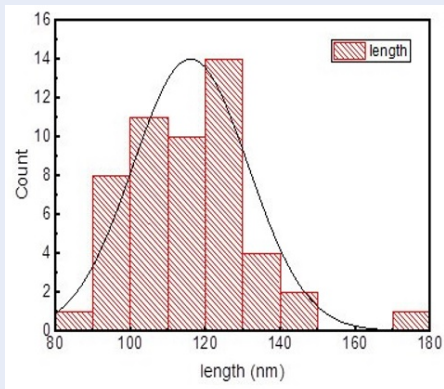
**Figure 1:** XRD pattern of ZnS nanoparticles (a) and ZnS nanoparticles decorated on SiO<sub>2</sub> nanospheres (b)

Figure 2 displays an SEM image of SiO<sub>2</sub>. The image reveals that SiO<sub>2</sub> exhibits a spherical morphology and uniform distribution with an average particle size of 115 nm (as depicted in Figure 3).



**Figure 2:** SEM image of SiO<sub>2</sub> nanospheres

SEM images of the ZnS nanoparticles showed that the ZnS nanoparticles aggregated with each other in the clusters (Figure 4). However, in the SEM image of SiO<sub>2</sub>@ZnS, the ZnS nanoparticles agglomerated on the surface of the SiO<sub>2</sub> nanospheres (Figure 5). Hence, SiO<sub>2</sub> nanospheres acted as templates for ZnS nanoparticle anchoring.



**Figure 3:** Particle size distribution histogram of SiO<sub>2</sub> nanospheres

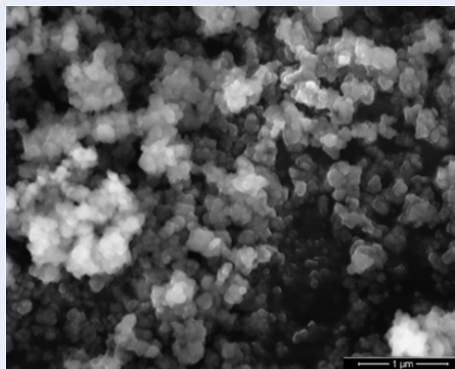


**Figure 4:** SEM image of ZnS nanoparticles

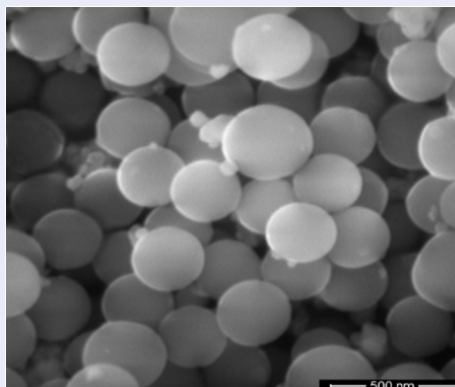


**Figure 5:** SEM image of S ZnS nanoparticles decorated on SiO<sub>2</sub> nanospheres

## UV-Vis absorption spectra of ZnS nanoparticles and SiO<sub>2</sub>@ZnS

Figure 6 shows the UV-Vis absorption spectra of the ZnS nanoparticles (a) and SiO<sub>2</sub>@ZnS (b). In the UV-Vis absorption spectrum of ZnS (Figure 6a), a prominent band appears with a maximum peak at 322 nm (3.85 eV), attributed to the near-band-edge absorption of ZnS<sup>19,20</sup>. This peak's maximum value demonstrates a blueshift compared to the 340 nm (3.65 eV) absorption peak of cubic bulk ZnS. Upon the addition of ZnS to the SiO<sub>2</sub> nanospheres, the absorption peak shifts to a longer wavelength of 328 nm (Figure 6b).

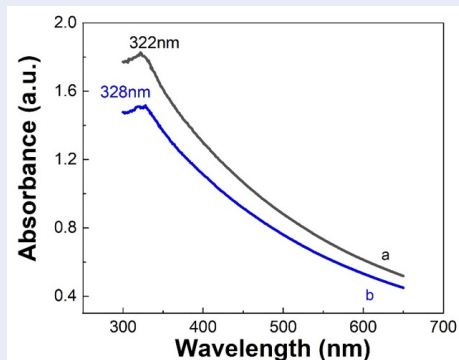
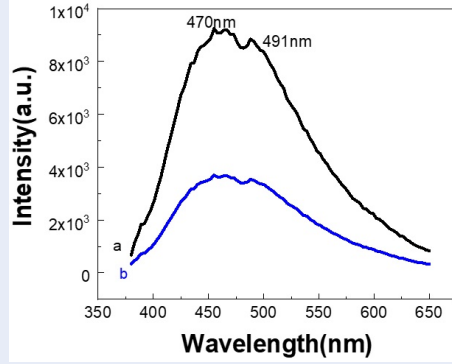


**Figure 6:** UV- Vis absorption spectra of ZnS nanoparticles (a) and ZnS nanoparticles decorated on SiO<sub>2</sub> nanospheres (b)

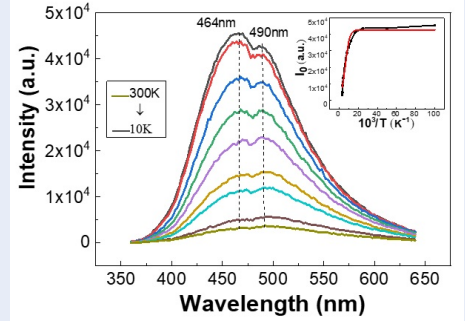
## PL spectra of ZnS nanoparticles and SiO<sub>2</sub>@ZnS

Figure 7 presents the PL spectra of both ZnS nanoparticles and SiO<sub>2</sub>@ZnS when excited by 325 nm radiation from a He-Cd laser at room temperature. At 300 K, there appears to be a broad luminescent band including two component bands at 470 and 491 nm (Figure 7a). These bands are attributed to defects in the crystal lattice, such as vacancies of zinc, sulfur, interstitial atoms of zinc, sulfur, and surface states<sup>21,22</sup>. When ZnS was decorated on SiO<sub>2</sub>, the intensity of these bands decreased significantly, while the peak positions of the two component bands shifted toward longer wavelengths at 472 and 494 nm (Figure 7b).

From the above results, we suppose that as-SiO<sub>2</sub> attaches to ZnS by the -NH<sub>2</sub> amin of APTMS; in addition to ZnS decorating SiO<sub>2</sub>, ZnS nanoparticles agglomerate together. Hence, the particle size of ZnS



**Figure 7:** PL spectra of ZnS nanoparticles (a) and ZnS nanoparticles decorated on SiO<sub>2</sub> nanospheres (b) at 300 K



**Figure 8:** Temperature-dependent PL spectra of ZnS nanoparticles when changing the measurement temperature from 300 to 10 K

increases, leading to a shift in the UV-Vis absorption and PL spectra of SiO<sub>2</sub>@ZnS toward longer wavelengths.

At 10 K, in the PL spectrum of the ZnS nanoparticles, there is also a broad band with two component bands at 464 and 490 nm assigned to defects in the ZnS crystal lattice, similar to that at 300 K. For SiO<sub>2</sub>@ZnS, at 10 K, there are bands at 440 and 482 nm, in which the 440 nm band has a strong intensity and the 482 nm band appears weakly on the right side of the 440 nm band. When the measurement temperature was increased from 10 K to 300 K, the position of the PL bands shifted toward longer wavelengths, and their intensity decreased rapidly (approximately 50 times) with temperature (Figures 8 and 9). The redshift of the PL spectra due to the energy band gap decreases with increasing temperature owing to exciton-phonon coupling and lattice deformation<sup>23,24</sup>.

The dependence of the luminescence intensity on temperature is as follows:

$$I(T) = \frac{I_0}{1 + A \exp\left(-\frac{E_A}{kT}\right)}$$

in which  $I_0$  is the PL intensity at 10 K

$A$  is a constant

$E_A$  is the activation energy

$k$  is the Boltzmann constant

From the dependence of the PL intensity on the measurement temperature ( $10^3/T$ ), the activation energies for ZnS (at 464 nm) and SiO<sub>2</sub>@ZnS (at 440 nm) were calculated to be 38 and 40 meV, respectively (refer to the inset in Figure 8 and Figure 9). These values are in agreement with references<sup>25,26</sup>. From the above results, it can be inferred that upon decorating

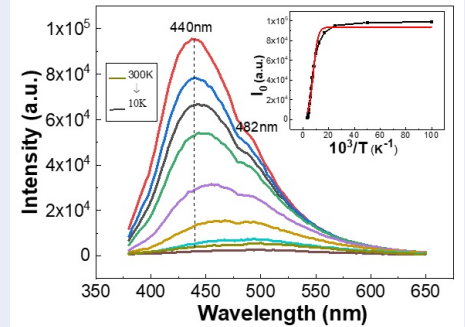


**Figure 9:** Temperature-dependent PL spectra of ZnS nanoparticles decorated on SiO<sub>2</sub> nanospheres when changing the measurement temperature from 300 to 10 K

ZnS on SiO<sub>2</sub> spheres, the surface states of ZnS undergo changes, resulting in subtle variations in both the UV-Vis and PL spectra, as well as the activation energy of ZnS.

## CONCLUSION

ZnS nanoparticles and ZnS nanoparticles decorated on SiO<sub>2</sub> nanospheres were successfully fabricated. The cubic-structured ZnS nanoparticles, averaging 2.8 nm in crystalline size, were decorated on SiO<sub>2</sub> nanospheres. Upon attachment of ZnS onto SiO<sub>2</sub> spheres, both the UV-Vis absorption and luminescence spectra exhibited a shift toward longer wavelengths, attributed to alterations in the surface states of ZnS. Notably, the luminescence spectra of ZnS and SiO<sub>2</sub>@ZnS increased by 50 times, while the position of the luminescent band shifted slightly when the measurement temperature decreased from 300 K to 10 K. The activation energies for ZnS and ZnS nanoparticles decorated on SiO<sub>2</sub> nanospheres



were determined to be 38 and 40 meV, respectively. These results are the basis for our further research on the photocatalysis and luminescence enhancement of ZnS nanoparticles decorated on SiO<sub>2</sub> templates.

## ACKNOWLEDGEMENTS

We extend our gratitude to the QG 22.15 project of Vietnam National University, Hanoi, for providing financial support for this paper.

## AUTHOR CONTRIBUTIONS

All the authors contributed to the study conception and design. Material preparation, data collection and analysis were performed by *Bui Hong Van, Nguyen Thi Bao Yen, Doan Thi Kim Dung, and Hoang Chi Hieu*. The first draft of the manuscript was written by *Bui Hong Van*, and all the authors commented on previous versions of the manuscript. All the authors have read and approved the final manuscript.

## COMPETING INTERESTS

The authors declare that they have no known competing financial interests or personal relationships that could have appeared to influence the work reported in this paper.

## REFERENCES

- Fang X, Zhai T, Gautam UK, Li L, Wu L, Bando Y, Golberg D. ZnS nanostructures: From synthesis to applications. *Prog Mater Sci*. 2011;56:175-287; Available from: <https://doi.org/10.1016/j.pmatsci.2010.10.001>.
- Liu H, Hu L, Watanabe K, Hu X, Dierre B, Kim B, Sekiguchi T, Fang X. Cathodoluminescence modulation of ZnS nanostructures by morphology, doping, and temperature. *Adv Funct Mater*. 2013;23:3701-3709; Available from: <https://doi.org/10.1002/adfm.201203711>.
- Ramasamy V, Praba K, Murugadoss G. Synthesis and study of optical properties of transition metals doped ZnS nanoparticles. *Spectrochim Acta A Mol Biomol Spectrosc*. 2012;96:963-971; PMID: 22938741. Available from: <https://doi.org/10.1016/j.saa.2012.07.125>.
- Kortan AR, Hull R, Opila RL, Bawendi MG, Steigerwald ML, Carroll PJ, Brus LE. Nucleation and growth of CdSe on ZnS quantum crystallite seeds, and vice versa, in inverse micelle media. *J Am Chem Soc*. 1990;112:1327-1332; Available from: <https://doi.org/10.1021/ja00160a005>.
- Kamat PV, Shanghavi B. Interparticle electron transfer in metal/semiconductor composites. Picosecond dynamics of CdS-capped gold nanoclusters. *J Phys Chem B*. 1997;101:7675-7679; Available from: <https://doi.org/10.1021/jp9709464>.
- Zhang Y, Li Y. Synthesis and characterization of monodisperse doped ZnS nanospheres with enhanced thermal stability. *J Phys Chem B*. 2004;108:17805-17810; Available from: <https://doi.org/10.1021/jp047446c>.
- Sarangi B, Mishra SP, Behera N. Advances in green synthesis of ZnS nanoparticles: An overview. *Mater Sci Semicond Process*. 2022;147:106723; Available from: <https://doi.org/10.1016/j.mssp.2022.106723>.
- Kozhevnikova NS, Melkozerova MA, Enyashin AN, Tyutyunik AP, Pasechnik LA, Baklanova IV, Suntsov AY, Yushkov AA, Buldakova LY, Yanchenko MY. Janus ZnS nanoparticles: Synthesis and photocatalytic properties. *J Phys Chem*

- Solids*. 2022;161:110459; Available from: <https://doi.org/10.1016/j.jpcs.2021.110459>.
- Singh S, Kaur V, Jyoti, Kumar N. Core-shell nanostructures: An insight into their synthetic approaches. In: *Metal Semiconductor Core - Shell Nanostructures for Energy and Environmental Applications*. 2017. p. 35-50; Available from: <https://doi.org/10.1016/B978-0-323-44922-9.00002-8>.
- Karar N, Chander H, Shivaprasad SM. Enhancement of luminescent properties of ZnS: Mn nanophosphors by controlled ZnO capping. *Appl Phys Lett*. 2004;85:5058-5060; Available from: <https://doi.org/10.1063/1.1815059>.
- Lu SY, Wu ML, Chen HL. Polymer nanocomposite containing CdS-ZnS core-shell particles: Optical properties and morphology. *J Appl Phys*. 2003;93:5789-5795; Available from: <https://doi.org/10.1063/1.1565830>.
- Ni M, Leung MKH, Leung DYC, Sumathy K. A review and recent developments in photocatalytic water-splitting using TiO<sub>2</sub> for hydrogen production. *Renew Sust Energ Rev*. 2007;11:401-425; Available from: <https://doi.org/10.1016/j.rser.2005.01.009>.
- Li Y, Ye C, Fang X, Yang L, Xiao Y, Zhang L. Fabrication and photoluminescence of SiO<sub>2</sub>-sheathed semiconducting nanowires: the case of ZnS/SiO<sub>2</sub>. *Nanotechnology*. 2005;16:501; Available from: <https://doi.org/10.1038/PhysRevB.75.041401>.
- Treccani L, Klein TY, Meder F, Pardun K, Rezwan K. Functionalized ceramics for biomedical, biotechnological and environmental applications. *Acta Biomater*. 2013;9:7115-7150; PMID: 23567940. Available from: <https://doi.org/10.1016/j.actbio.2013.03.036>.
- Mahajan J, Jeevanandam P. A facile thermal decomposition approach for the synthesis of SiO<sub>2</sub>@ZnS core-shell nanoparticles and their application as effective adsorbent for the removal of congo red. *Mater Today Commun*. 2021;26:102085; Available from: <https://doi.org/10.1016/j.mtcomm.2021.102085>.
- Ethiraj AS, Hebalkar N, Sainkar SR, Urban J, Kulkarni SK. Synthesis and investigation of ZnS nanoparticles adsorbed on functionalised silica particles. *Surf Eng*. 2004;20:367-372; Available from: <https://doi.org/10.1179/026708404225016391>.
- Dhas NA, Zaban A, Gedanken A. Surface synthesis of zinc sulfide nanoparticles on silica microspheres: sonochemical preparation, characterization, and optical properties. *Chem Mater*. 1999;11:806-813; Available from: <https://doi.org/10.1021/cm980670s>.
- Velikov KP, Blaaderen AV. Synthesis and characterization of monodisperse core-shell colloidal spheres of zinc sulfide and silica. *Langmuir*. 2001;17:4779-4786; Available from: <https://doi.org/10.1021/la0101548>.
- Jiang C, Zhang W, Zou G, Yu W, Qian J. Hydrothermal synthesis and characterization of ZnS microspheres and hollow nanospheres. *Mater Chem Phys*. 2007;103:24-27; Available from: <https://doi.org/10.1016/j.matchemphys.2007.02.007>.
- Niasari MS, Davar F, Mazaheri M. Synthesis and characterization of ZnS nanoclusters via hydrothermal processing from [bis(salicylidene)zinc (II)]. *J Alloys Compd*. 2009;470:502-506; Available from: <https://doi.org/10.1016/j.jallcom.2008.03.048>.
- Khosravi AA, Kundu M, Jatwa L, Deshpande SK, Bhagwat UA, Sastry M, Kulkarni SK. Green luminescence from copper doped zinc sulphide quantum particles. *Appl Phys Lett*. 1995;67:2702; Available from: <https://doi.org/10.1063/1.114298>.
- Dhas NA, Zaban A, Gedanken A. Surface synthesis of zinc sulfide nanoparticles on silica microspheres: sonochemical preparation, characterization, and optical properties. *Chem Mater*. 1999;11:806-813; Available from: <https://doi.org/10.1021/cm980670s>.
- Ramvall P, Tanaka S, Nornura S, Rblet P. Confinement induced decrease of the exciton-longitudinal optical phonon coupling in GaN quantum dots. *Appl Phys Lett*. 1999;75:1935-

- 332 1937;Available from: <https://doi.org/10.1063/1.124876>.
- 333 24. Wan JZ, Brebner JL, Leonelli R, Zhao G, Graham JT. Tem-  
334 perature dependence of free-exciton photoluminescence in  
335 crystalline GaTe. Phys Rev B Condens Matter. 1993;48:5197-  
336 5201;PMID: 10003788. Available from: <https://doi.org/10.1103/PhysRevB.46.1468>.
- 337
- 338 25. Nakamura S, Sakashita T, Yoshimura K. Temperature depen-  
339 dence of free exciton luminescence from high quality ZnS epi-  
340 taxial layers. Jpn J Appl Phys. 1997;36 ;Available from: <https://doi.org/10.1143/JJAP.36.L491>.
- 341
- 342 26. Tanaka M, Masumoto Y. Very weak temperature quenching in  
343 orange luminescence of ZnS: Mn<sup>2+</sup> nanocrystals in polymer.  
344 Chem Phys Lett. 2000;324:249-254;Available from: [https://doi.org/10.1016/S0009-2614\(00\)00587-X](https://doi.org/10.1016/S0009-2614(00)00587-X).
- 345